THE ASTROPHYSICAL JOURNAL, 308:954–965, 1986 September 15

EVIDENCE FOR NONLINEAR WAVE-WAVE INTERACTIONS IN SOLAR TYPE III RADIO BURSTS

R. P. LIN AND W. K. LEVEDAHL[1]
Space Sciences Laboratory, University of California at Berkeley
W. LOTKO
Thayer School of Engineering, Dartmouth College
D. A. GURNETT
Department of Physics and Astronomy, University of Iowa
AND
F. L. SCARF
TRW Defense and Space Systems, Redondo Beach, CA
Received 1984 November 30; accepted 1986 March 4

ABSTRACT

We present evidence that nonlinear wave-wave interactions occur in type III solar radio bursts. Intense, spiky Langmuir waves are observed to be driven by electron beams associated with type III solar radio bursts in the interplanetary medium. Bursts of 30–300 Hz (in the spacecraft frame) waves are often observed coincident in time with the most intense spikes of the Langmuir waves. These low-frequency waves appear to be long-wavelength ion acoustic waves, with wavenumber approximately equal to the beam resonant Langmuir wavenumber. Three possible interpretations of these observations are considered: modulational instability, parametric decay of the parent Langmuir waves to daughter ion acoustic and Langmuir waves, and decay to daughter electromagnetic waves and ion acoustic waves.

Subject headings: Sun: radio radiation — Sun: solar wind

I. INTRODUCTION

In this paper we present evidence for the nonlinear wave-wave interactions involving electrostatic electron plasma (Langmuir) waves in the solar wind, ion acoustic waves, and, possibly, transverse electromagnetic waves. The Langmuir waves are driven by electron beams associated with type III solar radio burst emission in the interplanetary medium. The electromagnetic waves may provide the type III radio emission near the electron plasma frequency, $f_{p-} \equiv \omega_{pe}/2\pi$.

The fast electrons are impulsively accelerated at the Sun, often in solar flares. As these electrons escape from the Sun, the faster ones will run ahead of the slower ones to produce locally a bump-on-tail velocity distribution. Langmuir waves are then excited at the local electron plasma frequency via the two-stream instability (Bohm and Gross 1949). Electron plasma waves with phase velocities corresponding to the positive slope portion of the bump will grow at the expense of the free energy in the bump. If the plasma waves grow rapidly enough, the bump will be flattened out, a process known as "quasi-linear relaxation" or "plateauing." For a spatially homogeneous beam-plasma model the fast particle beam is so rapidly diffused in velocity space by the intense plasma oscillations that a coherent stream would only be able to travel a few kilometers from its source before it is plateaued (Sturrock 1964). For type III bursts, however, the beam is spatially inhomogeneous, and velocity dispersion will tend to reform the bump that quasi-linear plateauing has flattened. Also, plasma waves produced with a given phase velocity may later be reabsorbed by the electron stream when the bump goes to lower velocities. A number of numerical computations of the quasi-linear evolution of the electron stream and of growth and reabsorption of the plasma waves have been done (Takakura and Shibahashi 1976; Magelssen and Smith 1977; Grognard 1982) which show that the stream will be able to propagate out at least to distances on the order of 1 AU. The numerical models predict electron distributions which are very plateau-like, and plasma wave levels which sometimes exceed the threshold for strong turbulence effects to become important (Nicholson *et al.* 1978; Goldman 1983).

Both plasma waves (Gurnett and Anderson 1976, 1977) and electrons (Lin 1970, 1974; Frank and Gurnett 1972; Lin, Evans, and Fainberg 1973) associated with type III bursts have been detected. Lin *et al.* (1981) presented the first measurements of the reduced (integrated over perpendicular velocities) parallel velocity distribution functions for the fast electrons associated with a type III radio burst at 1 AU. Detailed measurements of the plasma wave and radio emission were also presented for this burst. The electron distributions exhibit a well-defined bump-on-tail, with the bump progressing to lower velocities with time. In contrast to the expectations of quasi-linear models, however, there was no obvious plateauing of the bump; at a given parallel velocity significant positive slopes persisted for many minutes. The evolution of the observed Langmuir waves was qualitatively consistent with the variations of the electron distribution, but the wave levels were substantially below the level predicted from the electron distributions. These measurements indicate that the Langmuir waves were being shifted out of resonance with the electron beam.

Various nonlinear wave-wave interactions have been suggested for shifting the plasma waves out of resonance with the electron beam (see Goldman 1983, for review). These include induced scattering of the Langmuir waves off ion clouds

[1] Also Physics Department, University of California at Berkeley.

(Kaplan and Tsytovich 1968), parametric instabilities such as oscillating two-stream instability (Papadopoulos, Goldstein, and Smith 1974; Papadopoulos 1975; Smith, Goldstein, and Papadopoulos 1978; Goldstein, Smith, and Papadopoulos 1979; Freund *et al.* 1980), and strong turbulence processes such as soliton collapse (Zakharov 1972; Nicholson *et al.* 1978). In general, the dominant Langmuir wave transfer processes are those which involve a low-frequency excitation in addition to another Langmuir wave (Tsytovich 1970). For example, induced scattering, which occurs when $T_e \approx T_i$, can be viewed as the process of decay of the initial or pump Langmuir wave into an acoustic wave which is heavily damped, and another Langmuir wave (Bardwell and Goldman 1976). For $T_e > T_i$, the ion acoustic wave is more weakly damped, and this process becomes the parametric decay of the initial Langmuir wave into an ion acoustic wave and a daughter Langmuir wave. Another possibility is that density irregularities and ion acoustic waves already present in the solar wind can significantly affect the growth and saturation of beam-driven Langmuir waves, to the point of stabilizing the beam (Escande and de Genouillac 1978; Goldman and Du Bois 1982; Russell and Goldman 1983).

In this paper, we present the results of a search for low-frequency fluctuations in association with the Langmuir waves observed in type III radio bursts by the *ISEE 3* spacecraft. We find that waves with frequencies measured in the spacecraft frame of ~30–300 Hz commonly occur in coincidence with the strongest peaks of the Langmuir waves associated with the type III bursts.

II. OBSERVATIONS

The data used in this study were obtained from the *ISEE 3* spacecraft, which at the time of the observations was located in the solar wind $\sim 1.6 \times 10^6$ km (258 R_E) upstream from the Earth. The radio and plasma wave measurements are from the joint TRW-JPL-Iowa plasma wave instrument on *ISEE 3*, and the energetic electron measurements are from the University of California, Berkeley, solar electron instrument on *ISEE* 3. For a description of these instruments see Scarf *et al.* (1978), Anderson *et al.* (1978), and Lin *et al.* (1981).

Figure 1 shows a type III solar radio burst observed on 1979 March 11 with clearly associated Langmuir waves and energetic electrons. The top panel shows the spin-averaged electron fluxes detected by *ISEE 3*. The electron event begins at ~1050 UT for electrons of energies $\gtrsim$100 keV. Velocity dispersion is clearly evident, with the onset at the lowest observed energy of 2 keV occurring at ~1145 UT. Some energetic particles streaming upstream from the Earth's bow shock are also present in this time interval. These are especially noticeable at high energies at 1020–1025 UT and after ~1320 UT, but low-energy upstream electrons are also present sporadically throughout this interval.

The solar electrons appear to have been accelerated by an importance 2N solar flare located at S26 W77 in McMath plage region 15856 (*Solar Geophysical Data* 1979). A type III radio burst group of importance 2 was reported at metric wavelengths at 1036–1042.6 UT. Hard X-ray and microwave bursts were also observed from this flare.

The energetic electron data have been used to construct the reduced distribution of the electrons as a function of their velocity parallel to the magnetic field $f(v_\parallel)$. The Berkeley experiment provides measurements with $\Delta E/E \approx 12\%$ energy resolution from ~2 keV to ~1 MeV, and with 16 sector angular resolution in the ecliptic plane. We assume the electron distribution is symmetric about the magnetic field and integrate over $v_\perp$ for all particles with a given $v_\parallel$. The details of this procedure are described in Lin *et al.* (1981). Some representative $f(v_\parallel)$ distributions are shown in Figure 2*a*. The distributions for this event are similar to but less striking than those of the 1979 February 17 event reported by Lin *et al.* (1981). There is a strong nonthermal background prior to the event. As the flare electrons pass by the spacecraft, a bump-on-tail is developed from the faster flare electrons arriving before the slower ones. The positive slope ($\partial f/\partial v_\parallel > 0$) portion of the bump-on-tail is first observed at $v_\parallel = 5.5 \times 10^9$ cm s^{-1} at 1109 UT and continues down to $v_\parallel \approx 2.7 \times 10^9$ cm s^{-1} at 1142 UT. The typical range $\Delta v_\parallel$ which has $\partial f/\partial v_\parallel > 0$ is $\Delta v_\parallel/v_\parallel \approx 0.1$–$0.2$, and at a given $v_\parallel$ the distribution remains positive sloped for durations from 1 minute (the resolution of the measurement) to several minutes. Although this event is significantly less intense than the 1979 February 17 event, the positive $\partial f/\partial v_\parallel$ are still typically in the 10^{-26}–10^{-25} cm^{-5} s^2 range. In Figure 1 the times of $\partial f/\partial v_\parallel > 0$ are indicated at the top of the bottom panel. At the times of the most intense group of Langmuir waves (1137–38 UT) the positive slope portion is at $v_b \approx 3.5 \times 10^9$ cm s^{-1}, so the wavenumber $k_0 \approx \omega_{pe}/v_b \approx 2.3 \times 10^{-5}$ cm^{-1} for beam resonant Langmuir waves.

The bottom panel of Figure 1 shows the electric field intensities in 12 frequency channels from 17.8 Hz to 100 kHz. The black areas give the electric field intensities averaged over intervals of 32 s, and the solid lines give the peak field intensities over corresponding intervals. The smooth intensity variations characteristic of a type III radio burst, consisting of a rapid rise followed by a slow monotonic decay, are clearly evident in the 31.6, 56.2, and 100 kHz channels.

The very intense irregular electric field intensity variations in the 17.8 kHz channel from ~1110–1150 UT are electron plasma oscillations. Because of the filter overlap, electron plasma oscillations are also evident in the adjacent 10 kHz channel. The electron plasma frequency, f_{p-}, which is the characteristic frequency of the narrow-band electron plasma oscillations, is thus in between these two frequencies, in good agreement with the electron plasma frequency of 12.7 kHz computed using the plasma density of ~2 cm^{-3} (Table 1) measured by the solar wind plasma instrument on *ISEE 3* (Gosling 1984, private communication). The large difference between the peak and average electric field intensities indicates that the plasma oscillations are highly impulsive.

In the frequency range from ~3.16 kHz down to ~0.316 kHz there are highly bursty emissions occurring sporadically over the entire time interval. These have been previously identified as narrow-band, short-wavelength ion acoustic waves which are Doppler-shifted upward in frequency by the motion of the solar wind (Gurnett and Frank 1978). These emissions normally are observed at frequencies between the ion plasma frequency f_{p+} (~300 Hz here) and f_{p-} (Gurnett and Anderson 1977). The Langmuir waves appear to avoid times when these short-wavelength ion acoustic waves are present.

In this frequency range Figure 1 also shows some spurious wave activity. We refer to the weak 1 kHz and 560 Hz emissions with onsets near 1042. These signals (which are also barely detectable in the 316, 178, and 100 Hz channels) have amplitude versus time variations similar to those associated with high-frequency ($\gg$100 kHz) electromagnetic radiation characteristic of type III bursts. We believe that these signals are produced by a nonlinear distortion (down-conversion)

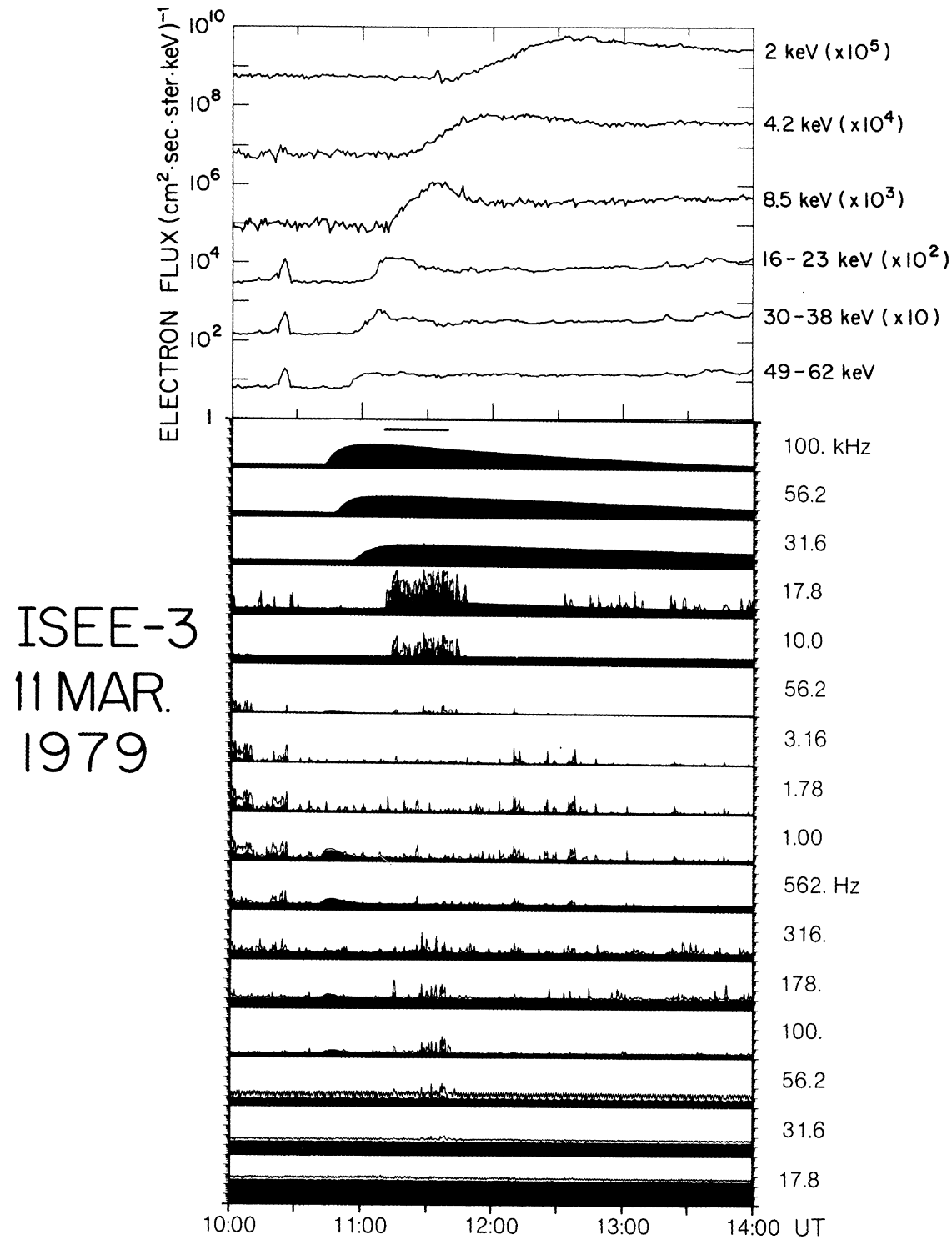

FIG. 1.—Top: spin-averaged flux of electrons from 2 to 62 keV for the type III solar radio burst of 1979 March 11. The spike at 1020 UT and smaller spikes which occur simultaneously in several energy channels are due to energetic particles flowing upstream from the Earth's bow shock. Velocity dispersion is clearly evident for the solar electrons. Bottom: electric field intensity measured in 16 broad-band channels from 100 kHz down to 17.8 Hz. Horizontal bar at the top indicates times of positive slope in the electron-reduced velocity distribution [$f(v_{\parallel})$]. Black areas show the average intensity over 32 s. Solid lines give the peak intensity. The smoothly varying profiles (100, 56.2, and 31.6 kHz) show the type III radio burst. The intense, highly impulsive emissions at 17.8 and 10 kHz are electron plasma waves. The sporadic bursty emissions between 3.16 kHz and $\sim$316 Hz have been previously identified as short-wavelength ion acoustic waves. The impulsive emissions at frequencies from 316 to 31.6 Hz which occur from $\sim$1115 to 1145 UT, simultaneous with the electron plasma waves, are believed to be long-wavelength ion acoustic waves.

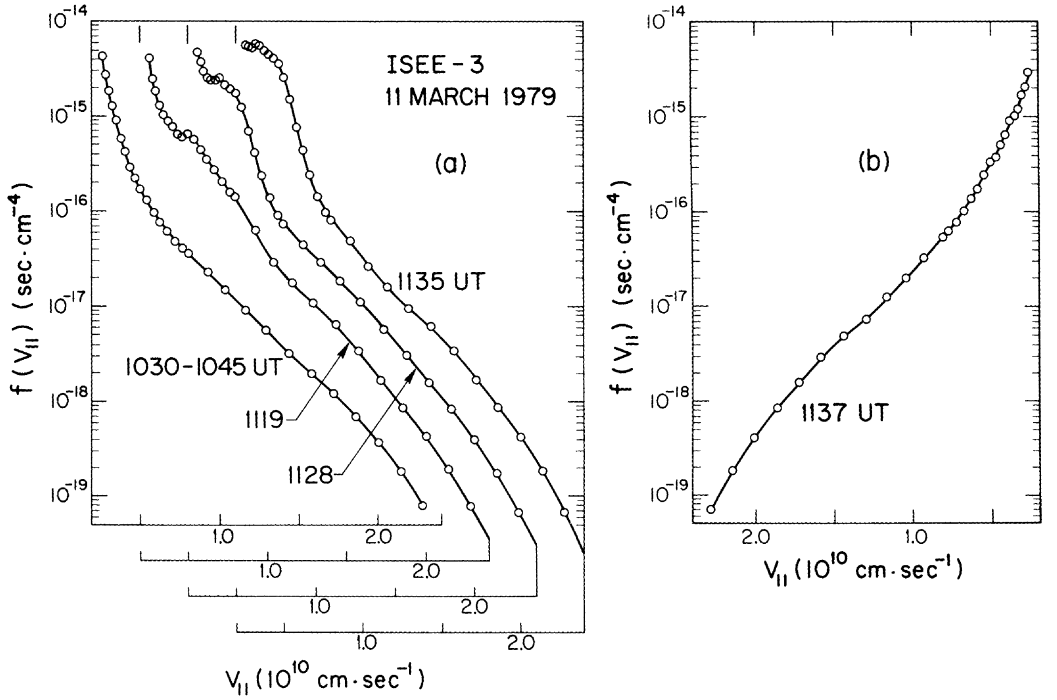

FIG. 2.—Examples of the one-dimensional velocity distribution functions obtained every 64 s during the 1979 March 11 solar electron event. (*a*) Pre-event nonthermal electron background averaged from 1030 to 1045 UT, as well as three 64 s distributions during the event, for electrons going away from the Sun. Each succeeding distribution is offset to the right by 5×10^9 cm s^{-1} (see bottom scale). Note the bump-on-tail which forms and moves to lower velocity with time. (*b*) Representative distribution for electrons in the backward direction (toward the Sun).

TABLE 1

PLASMA, BEAM, AND WAVE PARAMETERS

PARAMETERS	VALUES	
	1979 March 11	1979 February 8
Solar wind plasma:[a]		
Solar wind density, n	2 cm^{-3}	7
Solar wind velocity, V_{sw}	480 km s^{-1}	350
Angle of magnetic field to solar wind, θ_B	139°	63
Electron temperature, T_e	2×10^5 K	1.7×10^5
Ion temperature, T_i	$4 \times 10^{4\circ}$ K	6×10^4
Debye length, λ_D	2.2×10^3 cm	1.1×10^3
Electron plasma frequency, f_{p-}	13 kHz	24
Ion plasma frequency, f_{p+}	3×10^2 Hz	5.6×10^2
Fast electrons:		
Beam velocity, v_b	$\sim 3.5 \times 10^9$ cm s^{-1}	$\sim 3.5 \times 10^9$
Beam density, n_b	$\sim 7 \times 10^{-5}$ cm^{-3}	$\sim 2 \times 10^{-5}$
Positive slope, $\partial f/\partial v_\parallel$	$\sim 10^{-25}$ cm^{-3} s^2	$\sim 10^{-25}$
Beam width, $\Delta v_b/v_b$	~0.1–0.2	~0.1–0.2
Langmuir pump waves:		
Beam resonant wave number, k_0	2.3×10^{-5} cm^{-1}	4.3×10^{-5}
Maximum wave amplitude, $E_{0_{max}}$	~1 mV m^{-1}	~0.15
Maximum normalized energy density, $W_{max} = E_0^2/8\pi n\kappa T_e$	8×10^{-7}	6×10^{-9}
Long wavelength ion acoustic waves:		
Wavenumber, k_I (typical)	1.8×10^{-5} cm^{-1}	4×10^{-5}
Ion acoustic speed, c_s	5.2×10^6 cm s^{-1}	5.5×10^6
Ion acoustic frequency, f_I	15 Hz	35
Maximum electric field, $E_{I_{max}}$	~40 μV m^{-1}	~4

[a] Solar wind parameters provided by J. Gosling and W. Feldman, and magnetic field by B. Tsurutani, private communications (1984).

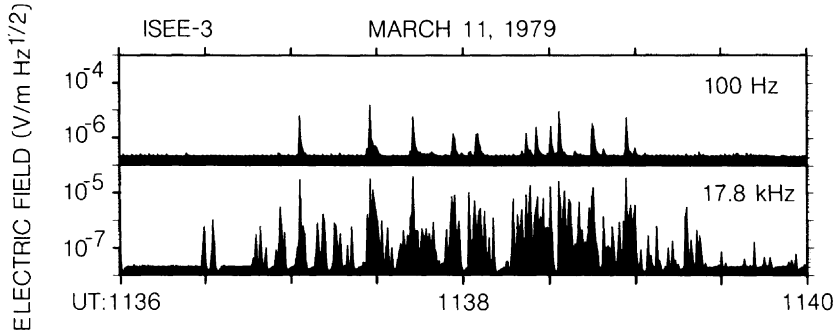

FIG. 3.—High-time resolution (0.5 s) plots of the Langmuir wave channel (17.8 kHz) and the 100 Hz long-wavelength ion acoustic wave channel for the 1979 March 11 event. Note the close correspondence between the most intense Langmuir wave spikes and the 100 Hz spikes.

within the preamplifier, driven by very intense electromagnetic waves in the MHz range.

From ~316 Hz down to 31.6 Hz there are highly impulsive bursts at the same time as the most intense bursts of Langmuir waves. In the 56.2 and 31.6 Hz channels, these are the only bursts detectable above the background. Since these low-frequency signals are correlated with the detection of very intense Langmuir waves in the 17.8 kHz channel, one might ask if these correlations are also spurious in the sense that the false "radio bursts" at 560 and 1000 Hz were simply instrumental by-products of intense MHz wave detection. This possibility can be ruled out, however, using data from the *ISEE 3* traversal of the geomagnetic tail. Within the tail we commonly detect comparable levels of auroral kilometric radiation in the 56 and 100 kHz channels, but these electromagnetic waves are never accompanied by signals such as the false "radio bursts." Thus we conclude that the correlation involving Langmuir waves and impulsive low-frequency bursts is a real one.

Figure 3 presents plots of the highest time resolution (0.5 s) data of the wave instrument for the 17.8 kHz Langmuir wave channel and the 100 Hz electric field channels for the period 1136–1140 UT. As reported previously (Gurnett and Anderson 1976; Lin *et al.* 1981), the Langmuir waves are extremely impulsive; intensity changes of over two orders of magnitude can occur within 0.5 s, and single bursts rarely last more than one or two 0.5 s readouts. There is no obvious asymmetry between rise and decay for the Langmuir wave bursts. The most intense of these bursts reach ~1 mV m^{-1}, more than three orders of magnitude above background. The *ISEE 3* plasma wave instrument has a receiver time constant of ~10 ms, and the peak amplitude in every 0.5 s is telemetered. Thus the peak wave amplitude is well determined, even for very spiky Langmuir waves. If the waves are confined to small spatial regions (such as solitons) then these regions would need to be much smaller than ~4 km, or ~250 λ_D, to be convected past the spacecraft too rapidly to be measured. Note that the wavelength of a beam-resonant Langmuir wave is ~2 km.

The close correlation of the low-frequency bursts to the Langmuir bursts is particularly clear in this figure. Most, but not all, of the Langmuir bursts which exceed ~0.1 mV m^{-1} are accompanied by a corresponding burst at 100 Hz. The maximum electric field at ~100 Hz is ~0.04 mV m^{-1}, almost two orders of magnitude above the background level. The fact that this low-frequency noise is not observed in the 100 Hz magnetic channel suggests that it is a low-frequency electrostatic mode, most likely a long-wavelength ion-acoustic wave. Similar low-frequency noise was observed upstream of the Jovian bow shock (Gurnett *et al.* 1981), but there the noise was present before the Langmuir waves appeared, and no obvious correlation with the Langmuir waves was reported. The 30–300 Hz low-frequency noise bursts observed here, however, are clearly not present prior to the Langmuir wave onset. Their close temporal correlation with the most intense Langmuir wave bursts suggests that they are the result of some nonlinear wave-wave interaction.

Representative spectra of these low-frequency bursts are shown in Figure 4. The bursts show broad peaks at $f_I \approx 100$ Hz and very rapid cutoff at high frequencies; the 1/10

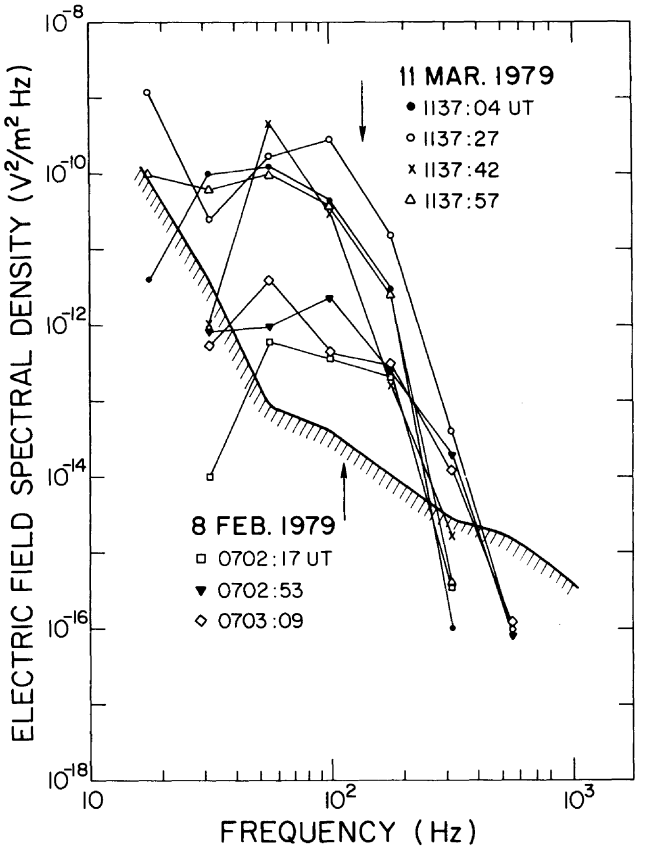

FIG. 4.—Spectra of the low-frequency bursts which are coincident with the intense Langmuir wave spikes. Background levels are shown by the hatched line. Each spectrum is taken at a single 0.5 s point. The arrows indicate the frequency at which ion acoustic waves would be observed in the spacecraft frame if they had wavenumber equal to that of the beam resonant Langmuir waves, i.e., $k_0 \approx \omega_{pe}/v_b$.

maximum point occurs at ~250 Hz. The frequency spectrum measured by the spacecraft is almost certainly determined by Doppler shifts, since the solar wind velocity is much larger than the phase velocity of all the known low-frequency electrostatic modes. If we assume that these are long-wavelength ion acoustic waves, Doppler-shifted by the solar wind velocity and aligned with the magnetic field, then their wavenumbers k_I are

$$k_I \approx \frac{2\pi f_I}{V_{sw} \cos \theta_B + c_s}, \quad (1)$$

where V_{sw} is the solar wind speed, c_s is the ion sound speed, and the angle between V_{sw} and the magnetic field is θ_B. For $f_I \approx 100$ Hz and the solar wind parameters in Table 1, $k_I \approx 1.8 \times 10^{-5}$ cm^{-1}. Note that these wavenumbers are comparable to the wavenumbers of the beam resonant Langmuir waves.

Figure 5 plots the low-frequency wave amplitude versus the Langmuir wave amplitude for the bursts shown in Figure 3. As mentioned earlier, there are a few intense bursts of Langmuir waves which appear to have little or no effect above background at low frequencies (points at bottom right). For most Langmuir bursts the electric field of the correlated low-frequency burst appears to increase approximately linearly with Langmuir wave amplitude.

Figure 6 shows a type III burst on 1979 February 8, with its associated energetic electron event and Langmuir waves. In this event the intensities of the Langmuir bursts are factors of 5–10 lower than in the 1979 March 11 event. The electrons appear to come from a $-N$ flare located at N08 W71 in McMath plage region 15802 (*Solar Geophysical Data* 1979). A type III radio burst group of importance 2 was reported at meter wavelengths at 0527.5–0528 UT, and a weak hard X-ray burst was also observed. Examples of $f(v_\parallel)$ for this event are shown in Figure 7. The nonthermal electron background is much lower here than in the 1979 March 11 event, so the evolution of the beam is more evident. The times of $\partial f/\partial v_\parallel > 0$ are indicated at the top of the bottom panel of Figure 6. In this event the Langmuir waves are most prominent in the 31.6 kHz channel, but are also observed in the adjacent 17.8 kHz channel. The solar wind density is ~7 cm^{-3}, which corresponds to $f_{p-} \approx 24$ kHz. Low-frequency (<300 Hz) noise is still observed coincident in time with the most intense Langmuir bursts (Fig. 8), but the amplitudes are correspondingly lower. The frequency spectra of the low-frequency noise for February 8 are similar to the spectra of 1979 March 11, with a similar cutoff at high frequency (Fig. 4). With the observed solar wind velocity and magnetic field angle (Table 1), the typical wavenumber for the low-frequency noise is $k_I \approx 4 \times 10^{-5}$ cm^{-1}. The beam resonant Langmuir waves also have wavenumbers $k_0 \approx 4 \times 10^{-5}$ cm^{-1}.

We have searched the *ISEE 3* data from launch in 1978 August to 1979 November for type III solar radio bursts at 1 AU with accompanying Langmuir wave bursts and fast electron events. A total of 39 events were found which were free from significant data gaps and contamination by upstream particles. Out of these 39 events, 29 showed evidence for low-frequency 30–300 Hz noise accompanying the intense Langmuir wave bursts. Three events had unusually high backgrounds in the low-frequency channels, and seven events had no obvious correlated low-frequency noise. Thus the presence of low-frequency 30–300 Hz noise coincident with the intense Langmuir wave spikes appears to be a common feature of type III solar radio bursts observed at 1 AU.

III. DISCUSSION

The plasma parameters for these two events are summarized in Table 1. Neglecting spontaneous emission and collisional damping, the growth of the Langmuir waves can be described

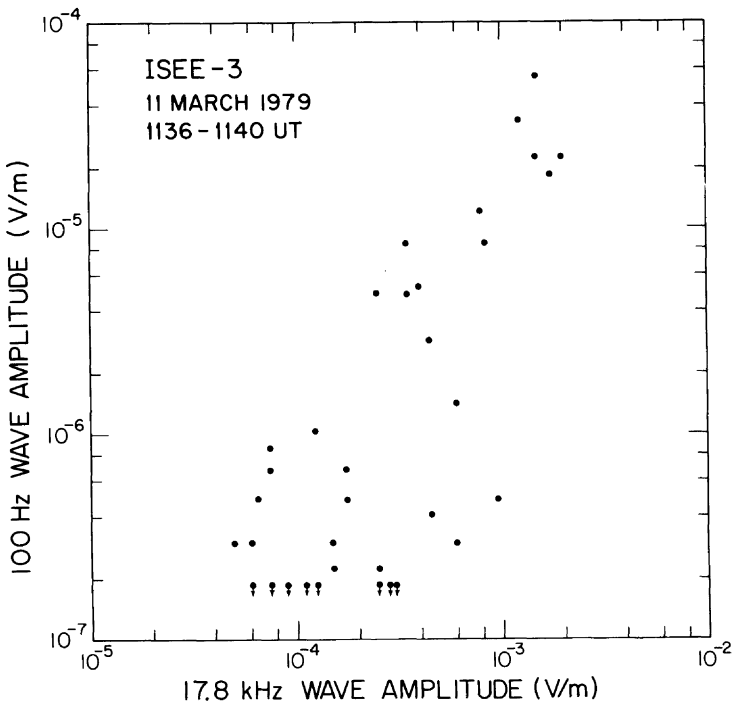

FIG. 5.—Peak electric field amplitude measured in the low-frequency (100 Hz) channel vs. the Langmuir wave (17.8 kHz) amplitude for the bursts of Fig. 3

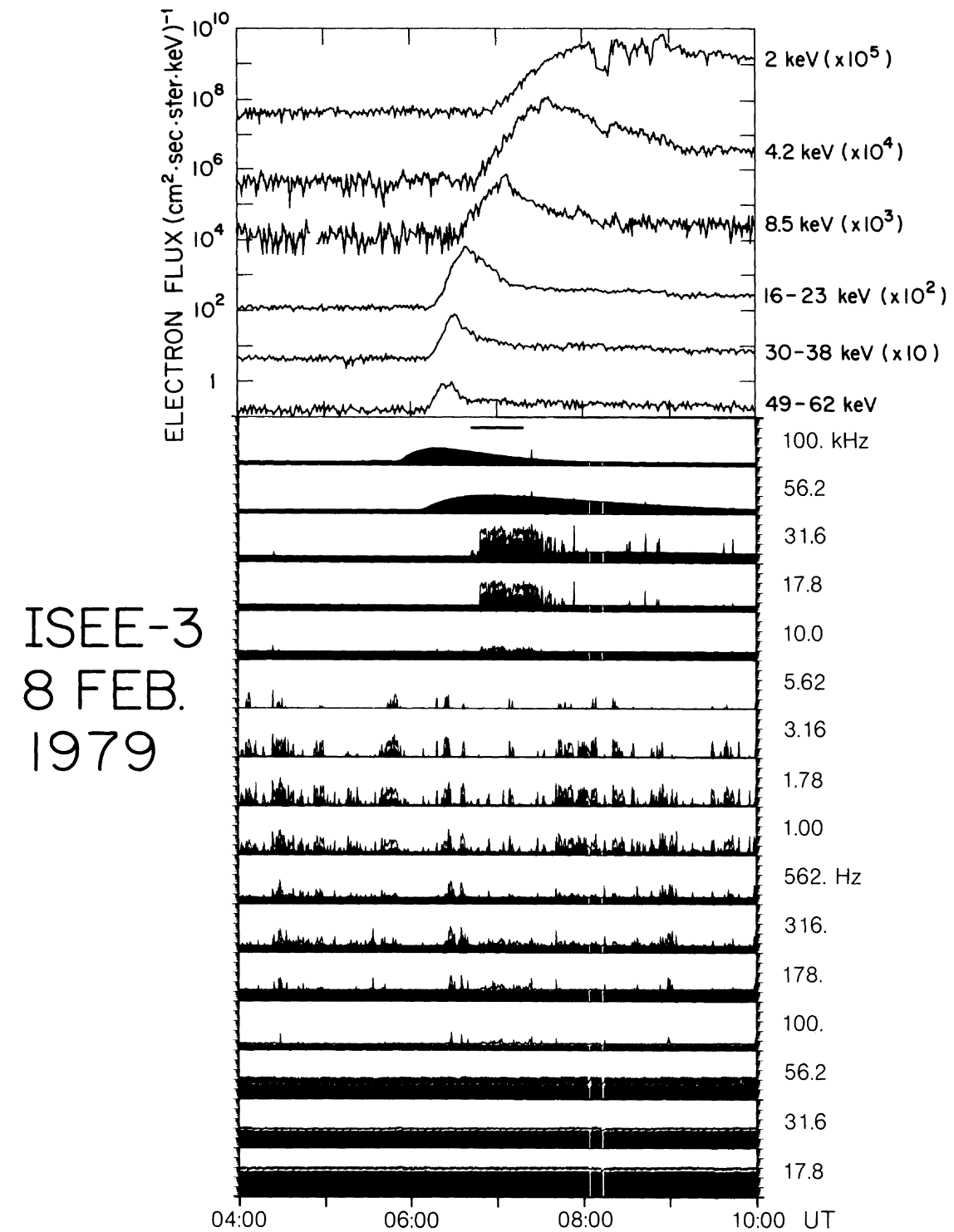

FIG. 6.—1979 February 8 type III burst event is shown here in the same format as Fig. 1. The Langmuir wave amplitudes here are 5–10 times lower than in the 1979 March 11 event.

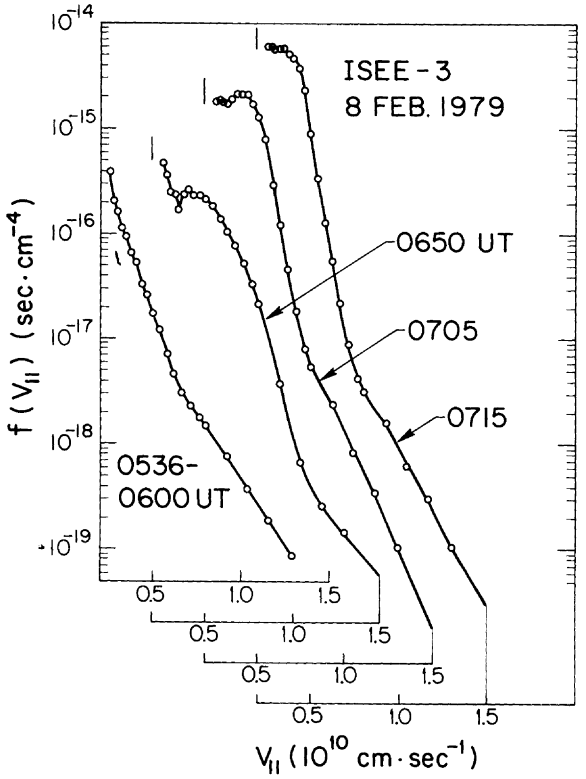

FIG. 7.—One-dimensional velocity distribution functions for 1979 February 8 event. The pre-event background (0536–0600 UT) is much lower for this event than for the 1979 March 11 event. Each succeeding distribution is offset to the right by 5×10^9 cm s^{-1} (see bottom scale).

in one dimension by

$$\frac{\partial P}{\partial t} = \gamma P(k, z, t) , \tag{2}$$

where

$$\gamma = \frac{4\pi^2 e^2 v_\parallel^2}{\omega m_e} \frac{\partial f}{\partial v_\parallel}\bigg|_{v_\parallel = \omega/k} \tag{3}$$

and $P(k, z, t)$ is the plasma wave energy distribution in wave-number k (Magelssen and Smith 1977). The large positive values of $\partial f/\partial v_\parallel$ observed in these events and in the 1979 February 17 event reported previously by Lin *et al.* (1981) give $\gamma \lesssim 1$ s^{-1}. Since $\partial f/\partial v_\parallel$ persists at these levels for minutes at a given velocity, linear theory for a homogeneous plasma would predict plasma wave levels many orders of magnitude above what is observed.

In addition, the observed distribution functions do not exhibit the strong plateauing predicted by quasi-linear models (Magelssen and Smith 1977; Grognard 1982). These observations indicate that some process is limiting the Langmuir wave growth. One possibility is that preexisting density irregularities or ion-acoustic waves in the solar wind could stabilize Langmuir wave growth and retard the beam relaxation process (Escande and de Genouillac 1978; Goldman and Du Bois 1982; Russell and Goldman 1983). The Langmuir waves do appear to be suppressed when the short-wavelength (300 Hz–3 kHz) ion acoustic noise bursts are present. For example, in Figure 6 the Langmuir wave levels drop at ~0709 UT when the 1–3 kHz bursts occur. Whistlers are sometimes present in the 1979 March 11 event. The Langmuir wave bursts appear to avoid these times as well. The electron angular distributions indicate that electrons are streaming back upstream from the Earth's bow shock toward the Sun at the times of the whistler waves. However, because these short-wavelength ion acoustic waves and whistler waves occur only sporadically, most of the spatial region filled by Langmuir waves is unaffected.

The close coincidence of the low-frequency (30–300 Hz) noise with the Langmuir wave bursts suggests that nonlinear wave-wave interactions are occurring. The low-frequency bursts show a marked asymmetry (Fig. 3); although in the 0.5 s resolution data the rise to peak in the 100 Hz bursts is unresolved, each burst clearly exhibits a decaying tail. These observed decays are most likely due to instrumental effects. If the low-frequency noise is associated with long-wavelength ion acoustic waves, then their damping rate can be calculated for the observed electron to ion temperature ratios (Table 1). From Fried and Gould (1961), the damping rate Γ_I for long-wavelength ion acoustic waves for typical $T_e/T_i \approx 4$ is given by $\Gamma_I/\omega_I \approx 0.1$, where ω_I is the ion acoustic frequency. For the March 11 and February 8 events, respectively, this implies damping rates of 9 s^{-1} and 22 s^{-1}. The fact that the associated damping times are fast suggests that some nonlinear process is maintaining the low-frequency fluctuations. However, such large damping rates place rather severe constraints on the possible nonlinear interactions.

At least three types of wave-wave interactions may be relevant: electrostatic modulational instability (Papadopoulos, Goldstein, and Smith 1974; Papadopoulos 1975; Smith, Goldstein, and Papadopoulos 1978; Goldstein, Smith, and Papado-

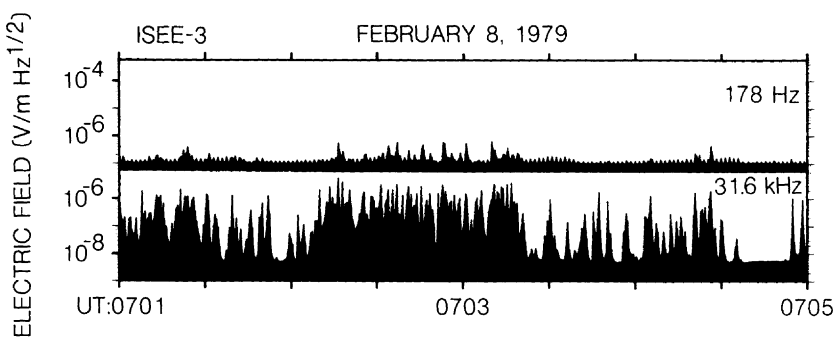

FIG. 8.—High-time resolution (0.5 s) plots of the Langmuir wave channel (31.6 kHz) and the 178 Hz long-wavelength ion acoustic wave channel for the 1979 February 8 event. Although the maximum Langmuir wave amplitude is about an order of magnitude lower than for 1979 March 11, closely correlated ion acoustic waves can be seen.

poulos 1978; Freund *et al.* 1980), or the decay instability of beam resonant Langmuir waves into daughter Langmuir waves and ion acoustic waves (Bardwell and Goldman 1976), or into daughter transverse waves and ion acoustic waves (Melrose 1980). We note here that a similar conclusion was drawn independently by Cairns (1986), based on these observations. Unlike the decay instabilities which are weak turbulence processes involving linear normal modes, the modulational instability involves an essentially zero-frequency ion quasi-mode, which does not satisfy a linear dispersion relation. To determine which if any of these processes may be occurring, we have used the data in Table 1 to evaluate their threshold intensities and the expected frequencies for the associated low-frequency fluctuations.

a) Modulational Instability

The threshold for modulational instability (neglecting dissipation) is given by (Sagdeev 1979)

$$W_{\rm th} > 3(\Delta k \lambda_{\rm D})^2 \tag{4}$$

where $W_{\rm th} = E_0^2/8\pi n\kappa T$ and Δk is the wavenumber half-width at half-maximum of the beam resonant Langmuir waves at the time of onset for modulational instability. The bandwidth Δk is related approximately to the range of initially unstable phase velocities Δv_b by

$$\frac{\Delta k}{k_0} = \frac{\Delta v_b}{v_b}\frac{\ln 2}{2N}, \tag{5}$$

where $k_0 \approx \omega_{pe}/v_b$ is the wavenumber of the maximally growing Langmuir wave, v_b is the electron beam velocity, and N is the number of linear growth times before the onset of modulational instability. Since the peak to background Langmuir wave intensity varies from $\sim 10^2$–10^3 in Figures 3 and 8, we estimate $N \approx 4.6$–6.9. Relations (5) and (4) and the parameters in Table 1 yield a threshold intensity $W_{\rm th} > 2 \times 10^{-7}$–$18 \times 10^{-7}$ for the 1979 March 11 event and $W_{\rm th} > 2 \times 10^{-7}$–$15 \times 10^{-7}$ for the 1979 February 8 event. The variation in these estimates is due to the uncertainties in the number of linear growth times N and the relative beam width, Δv_b, where $\partial f/\partial v_\parallel$ is positive. Although there is no self-consistent procedure for incorporating collisionless dissipation in the threshold criterion, we can reasonably expect the finite plasma dissipation to increase the above estimates. From Table 1, we find that the maximum observed intensity for the 1979 March 11 event is within the range of the calculated threshold, although the maximum intensity during the 1979 February 8 event is at least two orders of magnitude below the calculated threshold.

The frequency spectrum for the low-frequency fluctuations associated with modulational instability can be estimated from the Doppler-shifted wavenumber spectrum of a hyperbolic-secant-type Langmuir soliton. The soliton density fluctuation δn is given by (Nicholson 1983, pp. 180–181)

$$\frac{\delta n}{n} = \frac{-W_{\rm max}}{2}\,\mathrm{sech}^2\, k_0 x, \quad \text{where } k_0^2 \equiv \frac{W_{\rm max}}{12\lambda_{\rm D}^2}.$$

The Fourier transform of δn is

$$\frac{\delta n_k}{n} = \frac{-W_{\rm max}}{2k_0}\left(\frac{\pi k}{2k_0}\right)\mathrm{csch}\left(\frac{\pi k}{2k_0}\right). \tag{6}$$

The wavenumber spectrum is monotonic with a peak at $k = 0$; its intensity decreases to 1/10 of the peak value at $k = k_{0.1} \equiv 4.5(2k_0/\pi)$. Using the values in Table 1 for the March 11 event, this corresponds to a Doppler-shifted frequency of

$$f_{0.1} = \frac{k_{0.1}}{2\pi} V_{\rm sw} \cos\theta_B \approx 1.9 \text{ Hz}. \tag{7}$$

The rolloff frequency is below the 17.8 Hz instrument cutoff and well below the broad spectral peak in Figure 4 that extends from $\sim$30–100 Hz. Unless modulational instability produces collapsed structures significantly narrower than solitons, we conclude from the above estimate that it cannot account for the low-frequency fluctuations observed in either event.

Given this result, one may ask whether the observed plasma wave intensity could be artificially low by undersampling the signal. A larger energy density in the intensity of the plasma waves would result in narrower solitons whose Doppler-shifted frequency could conceivably explain the observed low-frequency noise. The plasma wave intensity will be underestimated if the transit time of the soliton past the spacecraft, $1/f_{0.1}$, is much less than the receiver time constant, $\tau_r = 10$ ms. Using the above values, this requires

$$W_{\rm max} \gg \left(\frac{4\pi^2\sqrt{3}}{9\cos\theta_B}\frac{\lambda_{\rm D}}{V_{\rm sw}\tau_r}\right)^2 \approx 2 \times 10^{-3}.$$

This intensity is many orders of magnitude greater than the observed intensity of 8×10^{-7}. Such large attenuation cannot be attributed to finite sampling by the receiver.

In summary, it appears unlikely that modulational instability is occurring during the 1979 February 8 event. A few of the most intense bursts during the 1979 March 11 event may be modulationally unstable, but the Doppler-shifted frequency associated with the resulting density cavities is 1–2 orders of magnitude too low to explain the observed low-frequency fluctuations.

b) Electrostatic Decay Instability

For decay instabilities involving a Langmuir pump wave at frequency and wavenumber ω_0, $\boldsymbol{k}_0$, an ion acoustic daughter wave at ω_I, $\boldsymbol{k}_I$, and a second daughter wave at ω_d, $\boldsymbol{k}_d$, conservation of wave energy and momentum imply

$$\boldsymbol{k}_0 = \boldsymbol{k}_d + \boldsymbol{k}_I, \tag{8}$$

and

$$\omega_0 = \omega_d + \omega_I. \tag{9}$$

In the long-wavelength regime appropriate for our measurements, the Langmuir pump and daughter ion acoustic waves satisfy the dispersion relations

$$\omega = \omega_{pe}(1 + \tfrac{3}{2}k^2\lambda_{\rm D}^2), \tag{10}$$

and

$$\omega_I = c_s k_I, \tag{11}$$

respectively, where $c_s = [(\kappa T_e + 3\kappa T_i)/m_i]^{1/2}$ is the ion acoustic speed. When the second daughter wave is a Langmuir wave, it also satisfies equation (10). In this case, the minimum threshold occurs when $\boldsymbol{k}_0$ and $\boldsymbol{k}_d$ are antiparallel, with $\boldsymbol{k}_I$ parallel to $\boldsymbol{k}_0$. Combining equations (8)–(11), we obtain

$$(k_0 - k_d)\lambda_{\rm D} \approx \frac{2}{3}\sqrt{\frac{m_e}{m_i}} = 0.016, \tag{12}$$

so

$$k_{I_{\max}} = k_0 + k_d \approx 2k_0 - \frac{0.016}{\lambda_D} \tag{13}$$

Assume a one-dimensional situation with $\boldsymbol{k}$ parallel to $\boldsymbol{B}$ for all the waves. The pump wave number k_0 is given by the requirement that it be resonant with the beam, $k_0 \approx \omega_{pe}/v_b$. From Table 1 we find that for the 1979 March 11 event $k_0 = 2.3 \times 10^{-5}$ cm^{-1} and $\lambda_D = 2.2 \times 10^3$ cm, so $k_{I_{\max}} = 3.9 \times 10^{-5}$ cm^{-1}. The maximum frequency for this ion acoustic wave (measured in the spacecraft frame) is then $f_{I_{\max}} = k_I V_{sw}/2\pi \cos \theta_B \approx 220$ Hz. This frequency corresponds to the observed cutoff in the frequency spectrum for the 1979 March 11 event (see Fig. 8). For the 1979 February 8 event we obtain $k_{I_{\max}} = 7.1 \times 10^{-5}$ cm^{-1} and $f_{I_{\max}} = 180$ Hz.

The daughter Langmuir waves have wavenumbers $k_d \approx 1.6 \times 10^{-5}$ and 2.8×10^{-5} cm^{-1} and phase velocities of 5×10^9 and 5.4×10^9 cm s^{-1} for the 1979 March 11 and February 8 events, respectively. These daughter waves will be traveling in the opposite direction from the pump waves, and thus will be damped by the high-energy tail of the backward (sunward) directed electron population. A representative reduced parallel velocity distribution function for that population is shown in Figure 2*b* (*left panel*). With the damping rates of the daughter Langmuir and ion acoustic waves we can compute the threshold W_0 for this decay process. From Bardwell and Goldman (1976) we obtain

$$W_0 = \frac{E^2}{8\pi n \kappa T} = 4\Gamma_L \Gamma_I/\omega_I \omega_p , \tag{14}$$

where Γ_L is the damping rate for the Langmuir daughter waves and Γ_I is the ion acoustic wave damping rate. Using $\Gamma_I/\omega_I \approx 0.1$ for the ion acoustic waves and Γ_L computed from equation (3) for the observed backward traveling electron distribution (Fig. 2*b*), we obtain $W_0 \approx 2.5 \times 10^{-5}$ and 7.5×10^{-8}, for March 11 and February 8, respectively. These values are about one to two orders of magnitude higher than the wave levels reached in those events, so parametric decay into a Langmuir daughter wave appears unlikely.

c) *Electromagnetic Decay Instability*

The pump Langmuir wave can also decay directly into a daughter transverse electromagnetic wave propagating perpendicular to the Langmuir wave and a daughter ion acoustic wave propagating nearly parallel to the Langmuir wave. This process may have been observed in the laboratory (Whelan and Stenzel 1981, 1985; see also Shukla *et al.* 1983) to produce radio emission at the fundamental. Using the dispersion relations for Langmuir (eq. [10]) and ion acoustic waves (eq. [11]) and for transverse waves ($k_T \ll w_p/c$),

$$\omega_T = \omega_{pe}(1 + \tfrac{1}{2}k_T^2 c^2/\omega_{pe}^2) , \tag{15}$$

and noting that $\omega_0 = \omega_T + \omega_I$ for this process, we obtain

$$\omega_{pe}(1 + \tfrac{3}{2}k_0^2 \lambda_D^2) = \omega_{pe}(1 + \tfrac{1}{2}k_T^2 c^2/\omega_{pe}^2) + c_s k_I . \tag{16}$$

Since $k_T \ll k_0$ and $\boldsymbol{k}_0 = \boldsymbol{k}_T + \boldsymbol{k}_I$, we have $k_0 \approx k_I$. For beam resonant Langmuir waves in the 1979 March 11 and February 8 events the resulting ion acoustic waves should have frequencies in the spacecraft frame of $\sim$130 and $\sim$110 Hz, respectively. These values are close to the peak of the observed low-frequency burst spectrum (Fig. 4).

The threshold for this process, under the assumption of an infinite homogeneous plasma, is given by Shukla *et al.* (1983) as

$$W_0 \gtrsim 4\Gamma_I \Gamma_T/\omega_I \omega_{pe} , \tag{17}$$

where Γ_I and Γ_T are the damping rates for the ion and electromagnetic waves, respectively. The Dawson-Oberman impedance (Dawson 1968) for a uniform high-frequency field is used to estimate the radiation absorption rate. Taking the ions to be either uncorrelated or thermally distributed we find

$$\frac{\Gamma_T}{\omega_{pe}} \lesssim \frac{2 \ln \lambda - 1}{\sqrt{18\pi\,\lambda}} , \tag{18}$$

where $\lambda = 4\pi n \lambda_D^3$.

The absorption rate would be somewhat greater if low-frequency ion fluctuations were present before the onset of the decay instability. If such fluctuations are present, they are not apparent within the uncertainties in our data. Relation (18), together with $\Gamma_I/\omega_I \approx 0.1$, yields a threshold the order of $W_0 \gtrsim 10^{-11}$ for both events in Table 1. This threshold is clearly exceeded by the observed Langmuir wave levels.

The maximum growth rate for the electromagnetic decay instability, neglecting geometrical effects, is given by Shukla *et al.* (1983) to within a factor of $(2)^{1/2}$ as

$$\Gamma_{NL} \equiv \mathrm{Im}\,(\Delta\omega) = \left(\omega_{pe}\omega_I \frac{W}{2}\right)^{1/2} , \tag{19}$$

Inserting the parameters for these events, we obtain nonlinear growth rates of 1.8 and 0.3 s^{-1}, respectively, for the March 11 and February 8 events. Since these are comparable with the linear growth rate for the electron beam instability, this process may detune the beam resonant Langmuir waves before quasi-linear diffusion processes relax the bump-on-tail distribution.

Goldman (1983) has pointed out that wave kinematics place an upper limit on the electron beam velocity. Frequency matching and the dispersion relations for the Langmuir, transverse, and sound waves imply

$$\frac{k_T^2}{k_0^2} = \frac{3v_e^2}{c^2}\left(1 - \frac{2}{3}\frac{c_s v_b}{v_e^2}\right), \tag{20}$$

when $k_I \approx k_0 \approx \omega_{pe}/v_b$. The solar wind electron thermal speed is defined as $v_e = (\kappa T_e/m_e)^{1/2}$. Since the expression in parentheses must be positive, we require $v_b < 1.5\, v_e^2/c_s$. This condition is satisfied for the two events examined here but may not hold in general. Relation (19) also places a lower limit on the wavelength of the transverse wave:

$$\lambda_T > \frac{1}{\sqrt{3}}\frac{2\pi}{k_0}\frac{c}{v_e} . \tag{21}$$

This lower limit is 260 and 150 km, respectively, for the 1979 March 11 and 1979 February 8 events.

The major difficulty with the electromagnetic decay interpretation is that the above analysis ignores convective effects and the solar wind inhomogeneity. Condition (17) above is sufficient to guarantee convective instability (Bers 1983). If the instability is convective, then the large group velocity of the electromagnetic waves may severely limit the growth of both the ion acoustic and transverse waves. It would be difficult in this case to interpret the observed low-frequency bursts in terms of an electromagnetic decay instability. Alternatively, if the electromagnetic wave energy is localized by solar wind

density fluctuations, then the instability may become absolute. Two possibilities for localization exist: wave trapping by refraction in large-scale density fluctuations (McDonald 1983) and wave localization by cumulative phase reinforcement due to multiple scattering by random, small-scale density fluctuations (Escande and de Genouillac 1984; Escande and Souillard 1984). These effects are difficult to quantify, however, given the uncertainty in the scale and structure of solar wind inhomogeneities, although some measurements have been made (Celnikier *et al.* 1983). In addition, neither process involves a simple mode-coupling process, so the usual criteria for distinguishing between convective and absolute instabilities in linearly inhomogeneous media (Bers 1983) cannot be used. A more definitive interpretation will clearly have to await further work on the convective and geometrical aspects of the instability.

The transverse waves from the electromagnetic decay instability may provide a natural source for type III radio burst emission at the fundamental, i.e., near f_{p-}. Assuming that convective effects do not severely limit the generation of transverse waves, we can estimate the intrinsic radio emissivity at the fundamental, since the Manley-Rowe relationships imply an equal rate of increase in the action densities of photons and ion acoustic waves:

$$\epsilon_{f_{p-}} = \frac{1}{4\pi}\frac{d}{dt}\left(\frac{E_T^2}{8\pi}\right) = \frac{2\Gamma_{\rm NL}}{4\pi}\frac{f_{pe}f_{pi}^2}{f_I^3}\frac{E_I^2}{8\pi}.$$

For the 1979 March 11 and 1979 February 8 events, we obtain maximum emissivities, respectively, of $\epsilon_{f_{p-}} \approx 10^{-15}$ and 10^{-18} W m^{-3} sr^{-1} during a spike. Since the intense spikes are observed only $\sim 1\%$ of the time, the average volume emissivity will be about two orders of magnitude lower. Note also that this fundamental radio emission occurs very close to f_{p-} and will be easily absorbed in surrounding regions of slightly higher density. Thus the level of radio emission observed far away from the source will likely be much lower than estimated from this emissivity. Gurnett, Anderson, and Tokar (1980) find the emissivity at 1 AU for 36 type III radio bursts to range from $\sim 10^{-26}$ to $\sim 10^{-21}$ W m^{-3} sr^{-1}, certainly consistent with the levels estimated here.

The identification of the type III radio emission as primarily fundamental (f_{p-}) radiation would also provide a consistent explanation for the observed timing between the radio emission and Langmuir waves. In type III events observed at 1 AU, the radio emission identified as originating near the spacecraft because of its lack of directivity was usually at frequencies near $2f_{p-}$. The onset of this "harmonic" radio emission typically *preceded* the Langmuir wave onset by 15–40 minutes. Lin *et al.* (1981) pointed out that this difficulty could be resolved if what was identified as harmonic radiation produced *in situ* could instead be fundamental radiation produced much closer to the Sun (see Kellogg 1980). Significant scattering of the fundamental radio emission off density irregularities would be required to explain the lack of directivity. Evidence that fundamental emission dominates from burst onset to peak and that scattering is important in the interplanetary medium has recently been presented (Dulk, Steinberg, and Hoang 1986; Steinberg *et al.* 1986).

IV. CONCLUSIONS

The observation of low-frequency (30–300 Hz) noise in close time coincidence with intense Langmuir wave bursts provides strong evidence for the occurrence of nonlinear wave-wave interactions during type III solar radio bursts. Of the three processes considered here, a decay instability of beam resonant Langmuir waves into transverse electromagnetic waves and ion acoustic waves would be most consistent with the observations, provided the electromagnetic wave energy is localized. Its threshold is below the observed Langmuir wave intensities, and the resulting ion acoustic waves would produce Doppler-shifted fluctuations in the observed frequency range. The threshold for decay of beam resonant Langmuir waves into daughter Langmuir waves and ion acoustic waves is much larger than the observed Langmuir wave intensities, so an electrostatic decay instability seems unlikely. The threshold for modulational instability may be exceeded only during a few of the most intense bursts of the 1979 March 11 event, but the associated density cavities produce Doppler-shifted fluctuations at frequencies well below the observed frequencies.

It is apparent that convective and geometrical effects are important considerations in this problem. Furthermore, localized spikes of Langmuir and ion acoustic waves lasting for only a few tenths of a second are observed. The short duration of the spikes is presumably due to the confinement of the waves to regions of scale size $L \lesssim 10^2$ km (Smith 1977), which are then convected past the spacecraft by the solar wind. This confinement is most likely due to inhomogeneities in the solar wind.

We wish to acknowledge useful discussions with M. Goldman, I. Cairns, P. Kellogg, D. Papadopoulos, T. Johnston, and D. Smith. We thank J. Gosling, W. Feldman, and B. Tsurutani for solar wind and magnetic field data. This research was supported at Berkeley in part by NASA grant NAG5-376, at Dartmouth College by NSF grant ATM-8445010, at Iowa by NASA contract NAS5-26819 and NASA grant NGL-16-001-043, and at TRW by JPL contract number 954012.

REFERENCES

Anderson, K. A., Lin, R. P., Potter, D. W., and Heetderks, H. D. 1978, *IEEE Trans. Geosci. Electron.*, **GE-16**, 153.
Bardwell, S., and Goldman, M. V. 1976, *Ap. J.*, **209**, 912.
Bers, A. 1983, in *Handbook of Plasma Physics*, Vol. **1**, ed. M. N. Rosenbluth and R. Z. Sagdeev, (Amsterdam: North Holland), p. 1.
Bohm, D., and Gross, E. P. 1949, *Phys. Rev.*, **75**, 1851.
Cairns, I. H. 1986, *Proc. Varenna Workshop on Plasma Astrophysics*, (ESA Pub. No.), in press.
Celnikier, L. M., Harvey, C. C., Jegou, R., Kemp, M., and Moricet, P. 1983, *Astr. Ap.* **126**, 293.
Dawson, J. M. 1968, *Adv. Plasma Phys.*, **1**, 1.
Dulk, G. A., Steinberg, J. L., and Hoang, S. 1986, *Astr. Ap.*, in press.
Escande, D. F., and de Genouillac, G. V. 1978, *Astr. Ap.*, **68**, 405.
Escande, D. F., and Souillard, B. 1984, *Phys. Rev. Letters*, **52**, 1297.
Frank, L. A., and Gurnett, D. A. 1972, *Solar Phys.*, **27**, 446.
Freund, H. P., Haber, I., Palmadesso, P., and Papadopoulos, K. 1980 *Phys. Fluids*, **23**, 518.
Fried, B. D., and Gould, R. W. 1961, *Phys. Fluids*, **4**, 139.
Goldman, M. V. 1983, *Solar Phys.*, **89**, 403.
Goldman, M. V., and Du Bois, D. F. 1982, *Phys. Fluids*, **25**, 1062.
Goldstein, M. L., Smith, R. A., and Papadopoulos, K. 1979, *Ap. J.*, **234**, 683.
Grognard, R. J.-M. 1982, *Solar Phys.*, **81**, 173.
Gurnett, D. A., and Anderson, R. R. 1976, *Science*, **194**, 1159.
———. 1977, *J. Geophys. Res.*, **82**, 632.
Gurnett, D. A., Anderson, R. R., and Tokar, R. L. 1980, in *IAU Symposium 86, Radio Physics of the Sun*, ed. M. R. Kundu and T. E. Gergely (Dordrecht: Reidel), p. 359.
Gurnett, D. A., and Frank, L. A. 1978, *J. Geophys. Res.*, **83**, 58.
Gurnett, D. A., Maggs, J. E., Gallagher, D. I., Kurth, W. S., and Scarf, F. L. 1981, *J. Geophys. Res.*, **86**, 8833.

Kaplan, S. A., and Tsytovich, V. N. 1968, *Soviet Astr—AJ*, **11**, 834.
Kellogg, P. J. 1980, *Ap. J.*, **236**, 696.
Lin, R. P. 1970, *Solar Phys.*, **12**, 266.
———. 1974, *Space Sci. Rev.* **16**, 189.
Lin, R. P., Evans, L. G., and Fainberg, J. 1973, *Ap. Letters*, **14**, 191.
Lin. R. P., Potter, D. W., Gurnett, D. A., and Scarf, F. L. 1981, *Ap. J.*, **251**, 364.
Magelssen, G. R., and Smith, D. F. 1977, *Solar Phys.*, **55**, 211.
McDonald, S. W. 1983, Ph.D. thesis, University of California, Berkeley.
Melrose, D. B. 1980, *Space Sci. Rev.*, **26**, 3.
Nicholson, D. R. 1983, *Introduction to Plasma Theory* (New York: Wiley).
Nicholson, D. R., Goldman, M. V., Hoyng, P., and Weatherall, J. C. 1978, *Ap. J.*, **225**, 605.
Papadopoulos, K. 1975, *Phys. Fluids.*, **18**, 1979.
Papadopoulos, K., Goldstein, M. L., and Smith, R. A. 1974, *Ap. J.*, **190**, 175.
Russell, D. A., and Goldman, M. V. 1983, *Phys. Fluids*, **26**, 2717.
Scarf, F. L., Fredricks, R. W., Gurnett, D. A., and Smith, E. J. 1978, *IEEE Trans. Geosci. Electron.*, **GE-16**, 191.
Sagdeev, R. Z. 1979, *Rev. Mod. Phys.*, **51**, 1.
Shukla, P. K., Yu, M. Y., Mohan, M., Varma, R. K., and Spatschek, K. H. 1983, *Phys. Rev. A*, **27**, 552.
Smith, D. F. 1977, *Ap. J. (Letters)*, **216**, L53.
Smith, R. A., Goldstein, M. L., and Papadopoulos, K. 1978, *Ap. J.*, **234**, 348.
Steinberg, J. L., Dulk, G. A., Hoang, S., Lecacheux, A., and Aubier, M. G. 1986, *Astr. Ap.*, submitted.
Sturrock, P. A. 1964, in *Proc. AAS-NASA Symposium on the Physics of Solar Flares*, ed. W. N. Hess (NASA SP-5), p. 357.
Takakura, T., and Shibahashi, H. 1976, *Solar Phys.*, **46**, 323.
Tsytovich, V. N. 1970, *Nonlinear Effects in Plasmas* (New York: Plenum).
Whelan, D. A., and Stenzel, R. L. 1981, *Phys. Rev. Letters*, **47**, 95.
———. 1985, *Phys. Fluids*, **28**, 958.
Zakharov, V. E. 1972, *Soviet Phys.—JETP*, **35**, 908.

D. A. GURNETT: Department of Physics and Astronomy, University of Iowa, Iowa City, IA 52242

W. K. LEVEDAHL and R. P. LIN: Space Sciences Laboratory, University of California, Berkeley, CA 94720

W. LOTKO: Thayer School of Engineering, Dartmouth College, Hanover, NH 03755

F. L. SCARF: TRW Systems, Building R-5, Room 1280, One Space Park, Redondo Beach, CA 90278